Electronic Supplementary Information

Catalyzing towards Clean Energy: Tuning Oxygen Evolution Reaction by Amide-Functionalized Co(II) and Ni(II) Pristine Coordination Polymers

Anup Paul,[a,*] Filipe Gusmão,[b] Abdallah G. Mahmoud,[a,c] Susanta Hazra,[a] Lazar Rakočević,[d] Biljana Šljukić,[b,e*] Rais Ahmad Khan,[f] M.Fátima C. Guedes da Silva,[a,g] Armando J. L. Pombeiro[a,*]

[a]Centro de Química Estrutural, Institute of Molecular Sciences, Instituto Superior Técnico, Universidade de Lisboa, Av. Rovisco Pais, 1049-001 Lisboa. Portugal
[b]Centro de Química-Física Molecular and IN-Institute for Nanosciences and Nanotechnologies and IBB-Institute for Bioengineering and Biosciences, Instituto Superior Técnico, Universidade de Lisboa, 1049-001 Lisboa, Portugal
[c]Department of Chemistry, Faculty of Science, Helwan University, Ain Helwan, Cairo 11795, Egypt
[d]Vinča Institute of Nuclear Sciences-National Institute of the Republic of Serbia, University of Belgrade, Mike Petrovića Alasa 12-14, 11000 Belgrade, Serbia
[e]CeFEMA, Instituto Superior Técnico, Universidade de Lisboa, 1049–001 Lisbon, Portugal.
[f]Department of Chemistry, King Saud University, Riyadh-11451, KSA
[g]Departamento de Engenharia Química,Instituto Superior Técnico, Universidadede Lisboa, Lisbon, Portugal

*Corresponding authors, E-mail:anuppaul@tecnico.ulisboa.pt, biljana@tecnico.ulisboa.pt, pombeiro@tecnico.ulisboa.pt

Contents:

Experimental Section

Materials and Physical Measurements

Solvents were dried and distilled prior to their use. 5-aminopyrimidine, terephthalic acid (TPA), thionyl chloride (SOCl$_2$), CoCl$_2$.6H$_2$O (98.0% purity), Ni(NO$_3$)$_2$.6H$_2$O (99.9% purity) were purchased from Sigma Aldrich Chemical Co. and used as received. Methyl-4-(chlorocarbonyl)benzoate was prepared following a procedure reported earlier.[29] FT-IR spectra were recorded on a Bruker Vertex 70 instrument in KBr pellets. ^{1}H (300 MHz) and ^{13}C (75.45 MHz) NMR spectra were obtained at room temperature (RT) on a Bruker Avance II + 300 (UltraShield^{TM}Magnet) spectrometer using tetramethylsilane [Si(CH$_3$)$_4$] as an internal reference. Carbon, hydrogen, and nitrogen elemental analyses were carried out by the Microanalytical Service of the Instituto Superior Técnico. Powder X-ray diffraction (PXRD) was conducted in a D8 Advance Bruker AXS (Bragg Brentano geometry) theta-2-theta diffractometer, with copper radiation (Cu Kα, λ = 1.5406 Å) and a secondary monochromator, operated at 40 kV and 40 mA. Flat plate configuration was used, and the typical data collection range was between 5˚ and 40˚. Thermal properties were studied using a Perkin-Elmer Instrument system (STA6000) at a heating rate of 10 ˚C min^{-1} under a dinitrogen

atmosphere flow rate of 30 mL/min. Gas sorption isotherms were measured at 77 K using a Micromeritics ASAP 2020 Surface Area Analyzer with prior degassing at 80 °C for 12 h. XPS analysis was performed using SPECS Systems with XP50M X-ray source for Focus 500 X-ray monochromator and PHOIBOS 100/150 analyzer. Source used was AlKα (1486.74 eV) anode at a 12.5 kV and 32 mA. Survey spectra (1000–0 eV binding energy) were recorded with constant pass energy of 40 eV, step size 0.5 eV and dwell time of 0.2s in the FAT mode. High resolution spectra of Ni 2p and Co 2p were recorded at a constant pass energy of 20 eV, step size of 0.1 eV and dwell time of 2s. All energy positions were referenced to C1s at 284.8 eV.

Synthesis of 4-(pyrimidin-5-ylcarbamoyl)benzoic acid (HL)

In a two-fold synthetic procedure, the pro-ligand **HL** was successfully generated (Scheme S1). The initial step involved the gradual addition of methyl-4-(chlorocarbonyl)benzoate (1.98 g, 10.0 mmol) dissolved in 30 mL of tetrahydrofuran (THF) to a solution of 5-aminopyrimidine (0.94 g, 10.0 mmol) in 30 mL THF. The resulting mixture was subjected to stirring for 24 h. Subsequently, the solvent was removed using a rotary evaporator until complete dryness. The resultant crude product underwent recrystallization utilizing methanol (MeOH), leading to the isolation of the pure product denoted as **LMe**.

In the subsequent phase of the synthesis, the **LMe** underwent hydrolysis, following a documented protocol,[29–31] resulting in the successful isolation of the desired pro-ligand **HL**. Yield: 1.9g (65%). Anal. Calcd for $C_{12}H_9N_3O_3$: C, 59.26; H, 3.73; N, 17.28. Found: C, 560.09; H, 3.69; N, 17.33. FT-IR (KBr, cm^{-1}): 1700(s), 1546(s), 1422(s), 1279(s), 1116(w), 906(w), 785(w), 711 (s). ^{1}H-NMR (400 MHz, DMSO-d_6, δ ppm): 13.32 (s, 1H, COOH), 10.81 (s, 1H, NH), 9.18 (s, 1H, H$_{py}$), 8.96 (s, 1H, H$_{py}$), 8.13 (m, 4H, Ar-H), 8.04 (s, 1H, H$_{py}$). ^{13}C-NMR (77 MHz, DMSO-d_6, δ ppm): 167.13, 165.87, 154.04, 148.79, 134.90, 134.33, 130.07, 128.56. ESI-MS: m/z [(M + H)]$^+$, Calcd. 243.07, found 243.12, [(M + Na)]$^+$, Calcd. 265.07, found 264.95.

Synthesis of [Co(L)$_2$(H$_2$O)$_2$]$_n$ (Co-CP)

HL (10 mg, 0.041 mmol) was dissolved in 1 mL DMF, while Co(NO$_3$)$_2$.6H$_2$O (24 mg, 0.082 mmol) was dissolved separately in 1 mL H$_2$O. These solutions were mixed in an 8 mL glass vial which was then sealed securely. After 24 h of heating at 75°C distinctive pink crystals of compound **Co-CP** were produced in the reactor. These crystals were cooled, isolated, and subjected to washing with deionized water and DMF, followed by air drying; they were suitable for singe crystal X-ray diffraction analysis. Yield: 60% Anal. Calcd for $C_{24}H_{20}CoN_6O_8$: C, 49.75; H, 3.48; N, 14.51. Found: C, 49.82; H, 3.53; N, 14.47. IR

(KBr/pellet, cm^{-1}): 3152 (br), 1679 (w), 1592 (w), 1530 (s), 1431 (w), 1373 (s), 1282 (s), 901(w), 806 (w), 720 (w), 645(w).

Synthesis of [Ni(L)$_2$(H$_2$O)$_2$]$_n$ (Ni-CP)

Following a methodology akin to that utilized for compound **Co-CP**, we applied a parallel procedure involving **HL** (10 mg, 0.041 mmol) and Ni(NO$_3$)$_2$.6H$_2$O (25 mg, 0.086 mmol) dissolved in a mixture of DMF and H$_2$O (1 mL each). The ensuing outcome led to the formation of distinctive green crystals for compound **Ni-CP**, suitable for single crystal X-ray diffraction analysis. Yield: 65%. Anal. Calcd for C$_{24}$H$_{20}$N$_6$NiO$_8$: C, 49.77; H, 3.48; N, 14.51. Found: C, 49.98; H, 3.52; N, 14.49. IR (KBr/pellet, cm^{-1}): 3143 (w, br), 1683 (m), 1588 (w), 1530 (s), 1373 (w), 1265 (w), 893 (w), 635 (w).

Synthesis of the heterobimetallic CoNi-CP

A mixture of Ni(NO$_3$)$_2$·6H$_2$O (0.85 mmol, 241 mg) and Co(NO$_3$)$_2$·6H$_2$O (0.85 mmol, 241 mg) in methanol (8 mL) was added to a solution of the ligand **HL** (0.85 mmol, 213 mg) dissolved in 8 mL of DMF, 8 mL of methanol and 4 mL of water. The obtained solution was charged in a closed glass vial and kept at 80 ^{o}C for 3 days. The obtained off pink crystalline material (194 mg) was isolated by filtration, washed with diethyl ether and dried under vacuum. ICP (%): Ni 5.8, Co 5.5. FT-IR (KBr): ν (cm^{-1}) = 1691 m, 1591 w, 1577 m, 1530 s, 1434 s, 1407 w, 1370 m , 1332 w, 1310 w, 1282 m, 1185 m, 1125 m, 1088 m, 1016 m, 974 w, 959 w, 917 m, 900 m, 878 m, 827 m, 800 m, 739 s, 719 s, 679 s, 647 s, 556 w, 526 m, 462 w, 442 s, 415 w.

Crystal Structure Determination

X-ray quality single crystals of **Co-NP** and **Ni-CP** were immersed in cryo-oil, mounted in a nylon loop and measured at room temperature. Intensity data were collected using a Bruker Bruker APEX-II PHOTON 100 diffractometer. Bruker SMART software was used to retrieve cell parameters and Bruker SAINT for refinement.[1,2] Both structures were solved by direct methods and refined using SHELXL-2019/3.[3] Calculations were performed using the WinGX System-Version 2018.3.[4] Crystallographic data are summarized in Table S1 and selected bond distances, angles and relevant hydrogen bond contacts are shown in Table S2 and S3, ESI. CCDC deposition Nos. 2308477 and 2308478, respectively, which contain the supplementary crystallographic data for this paper. These data can be obtained free of charge from The Cambridge Crystallographic Data Centre *via* www.ccdc.cam.ac.uk/data_request/cif.

A suitable X-ray diffraction quality crystal of **CoNi-CP** was not obtained after several synthetic attempts.

Electrochemical measurements

The electrochemical measurements were done for **Co-CP**, **Ni-CP** and the heterometallic **CoNi- CP**. The working electrodes were prepared using a slurry made of catalytic material, and Nafion™ binder in the mass ratio of 63:1. The slurries were prepared mixing the previously ground CPs with the binder in water (600 µL) and ethanol (400 µL) mixture. 5 µL of the resulting mixture was then coated onto a glassy carbon substrate (4 mm diameter) and dried at 50 °C for 15 min in an electric oven.

The electrochemical measurements were performed in a standard three-electrode electrochemical cell using a platinum coil as the counter electrode, a saturated calomel electrode (SCE) as the reference electrode and a working electrode described above. All potential values are shown with respect to the reversible hydrogen electrode (RHE).

All measurements were done in a 1 M KOH electrolyte. For capacitance measurements, cyclic voltammetry (CV) was carried out in nitrogen-saturated electrolyte in the open circuit potential region. Electrochemical impedance spectroscopy (EIS) measurements were carried out in a frequency range from 100 kHz to 0.1 Hz. Linear sweep voltammetry (LSV) measurements at 10 mV s^{-1} were used to evaluate the material activity toward oxygen evolution reaction. Durability tests were carried out in switch mode, i.e., holding the potential at 1.7 V for 30 s followed by a reduction potential for 120 s to clean the electrode surface from the evolved gas bubbles. All electrochemical measurements were performed using an ALS/DY2325 Bi-Potentiostat from ALS Japan.
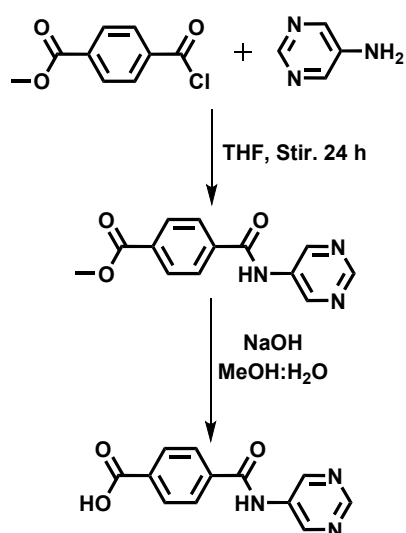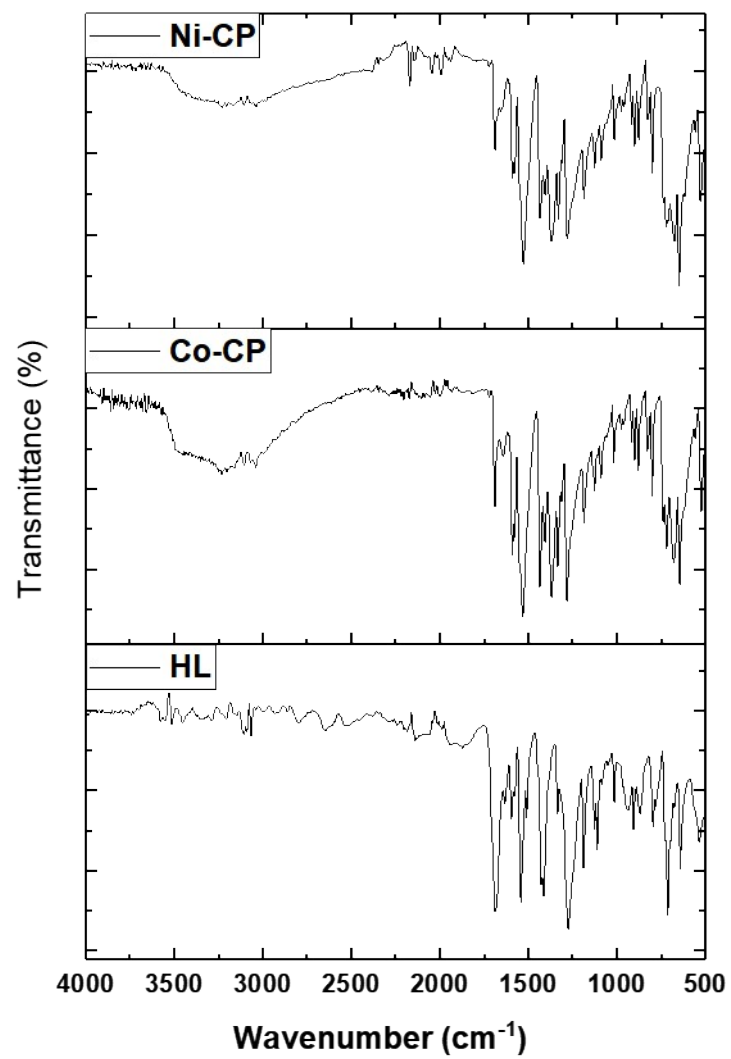

Scheme S1: Synthesis of **HL.**
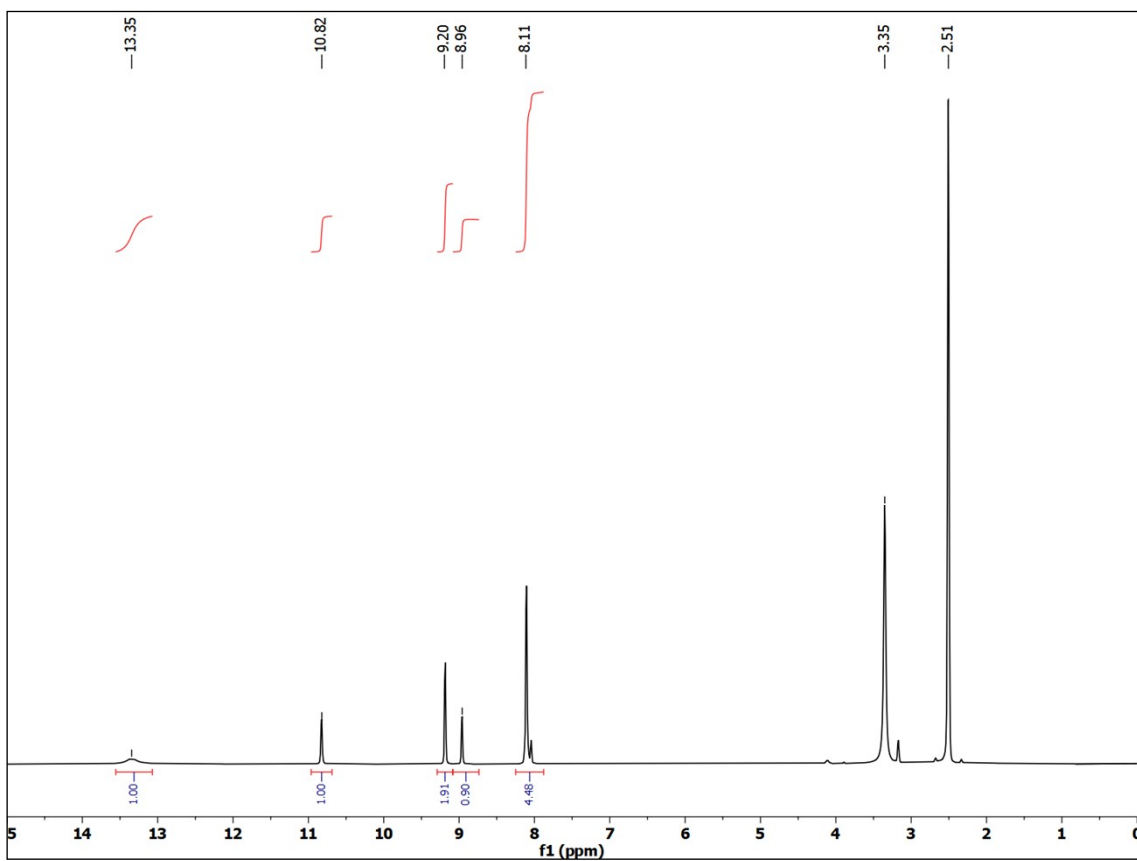
Figure S1: ATR-IR spectra of **HL, Co-CP** and **Ni-CP.**

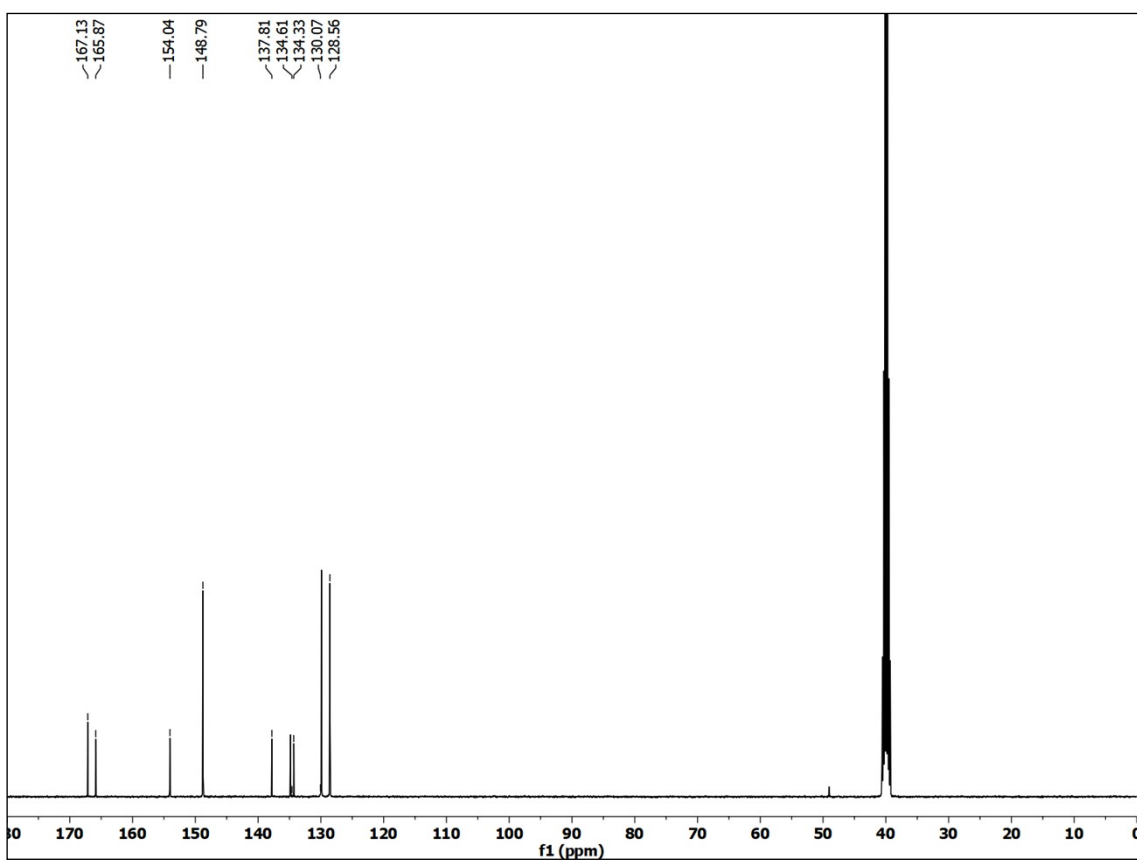**Figure S2.** ^{1}H-NMR spectrum of **HL** recorded in CDCl$_3$.

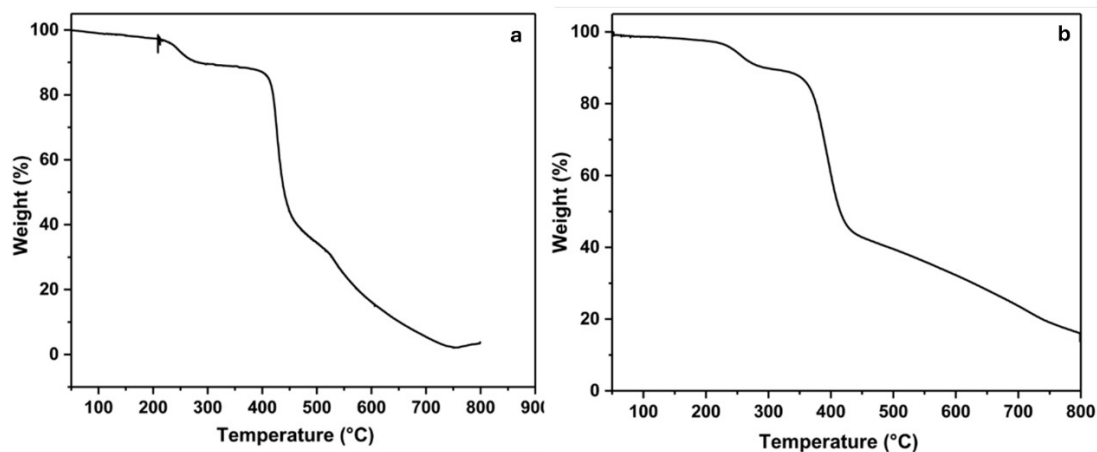**Figure S3.** ^{13}C-NMR spectrum of **HL** recorded in CDCl$_3$.
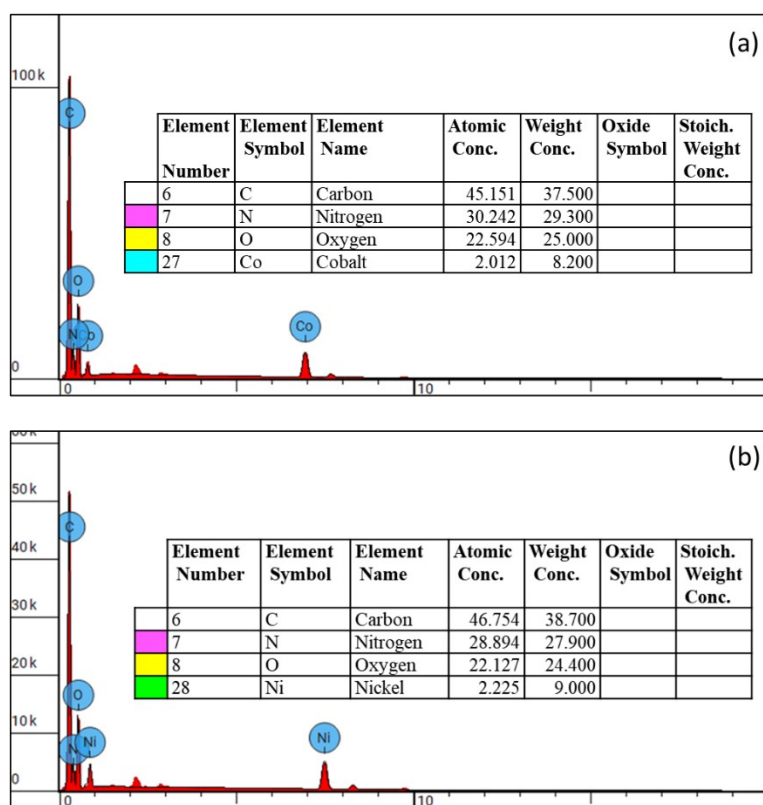

Figure S4: TGA of **Co-CP** (a) and **Ni-CP** (b).

Element Number	Element Symbol	Element Name	Atomic Conc.	Weight Conc.	Oxide Symbol	Stoich. Weight Conc.
6	C	Carbon	45.151	37.500		
7	N	Nitrogen	30.242	29.300		
8	O	Oxygen	22.594	25.000		
27	Co	Cobalt	2.012	8.200		

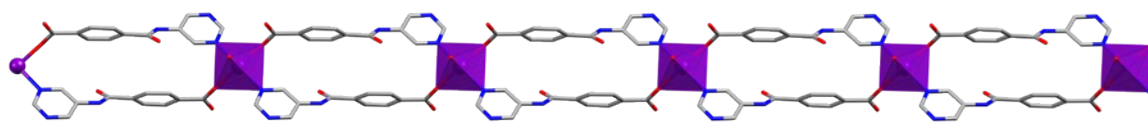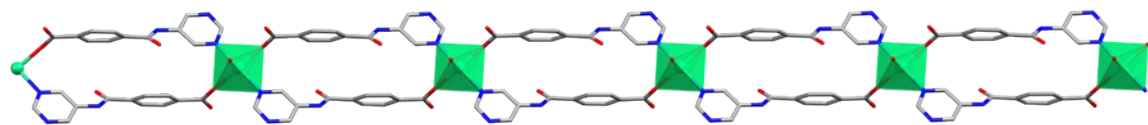| Element Number	Element Symbol	Element Name	Atomic Conc.	Weight Conc.	Oxide Symbol	Stoich. Weight Conc.
6	C	Carbon	46.754	38.700		
7	N	Nitrogen	28.894	27.900		
8	O	Oxygen	22.127	24.400		
28	Ni	Nickel	2.225	9.000		

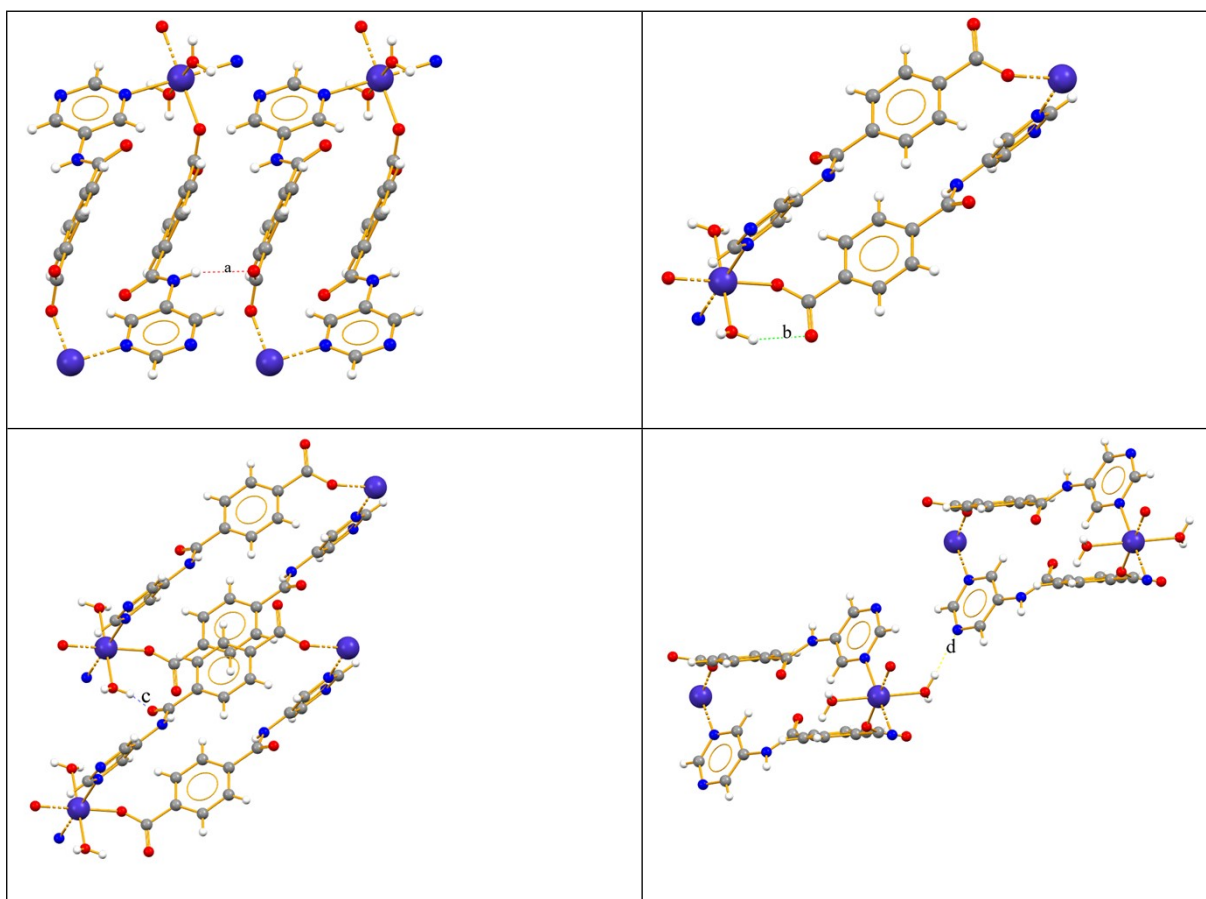**Figure S5:** EDX of CPs **Co-CP** (a) and **Ni-CP** (b).

(a)

(b)

Figure S6. Polyhedral representation of the loop chain-like one-dimensional network in **Co-CP** (a) and **Ni-CP** (b). All H-atoms are omitted for clarity.
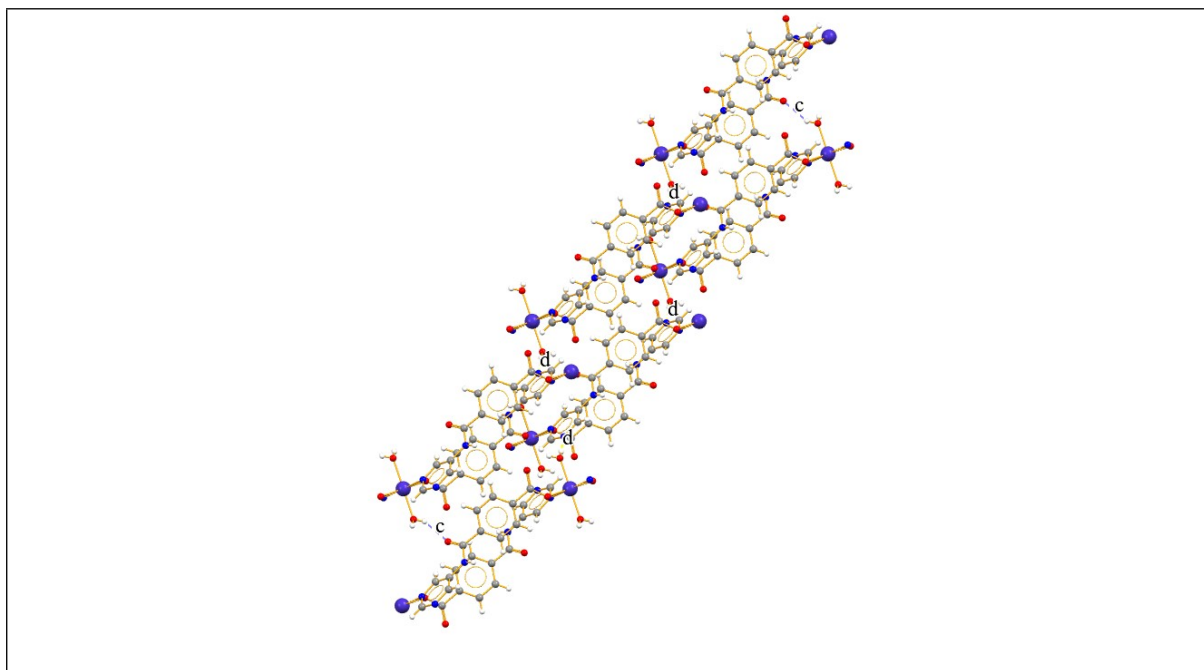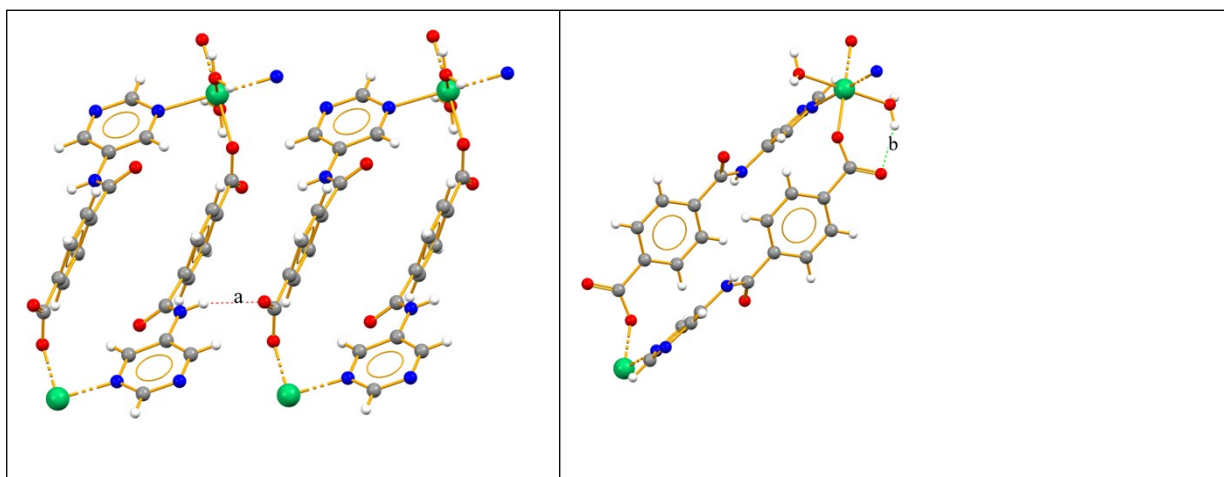
Figure S7a. First level H-bonds graph set representations present in **Co-CP**, and their respective descriptors: (*a*) $C_1^1(9)$ between N_{amide} and the $O_{carboxylate}$; (*b*) $S_1^1(6)$; (*c*) $C_1^1(9)$ between O_{water} and the O_{amide}; and (*d*) $C_1^1(14)$ between O_{water} and the $N_{pyrimidine}$. One of the highest second level interactions (bottom) is also shown, the $R_2^2(82)$ one involving contacts *c* and *d*.
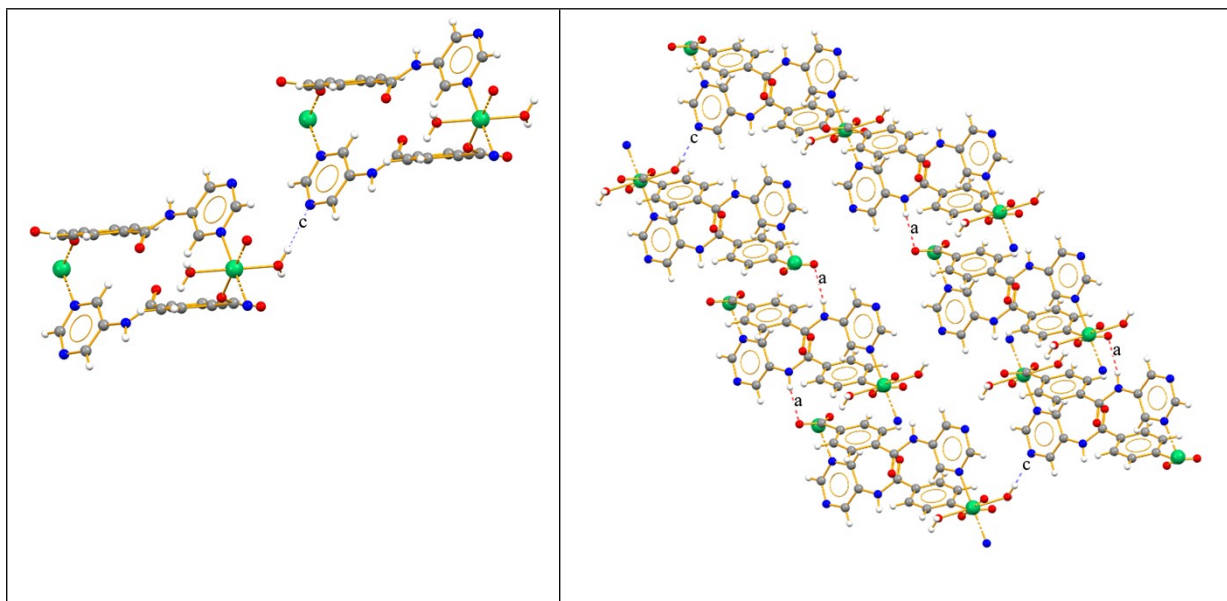
Figure S7b. First level H-bonds graph set representations present in **Ni-CP**, and their respective descriptors: (*a*) $C_1^1(9)$ between N_{amide} and the $O_{carboxylate}$; (*b*) $S_1^1(6)$; (*c*) $C_1^1(9)$ between O_{water} and the $N_{pyrimidine}$. One of the highest second level interactions (bottom) is also shown, the $R_2^2(88)$ one involving contacts *a* and *c*.

(a)   (b)
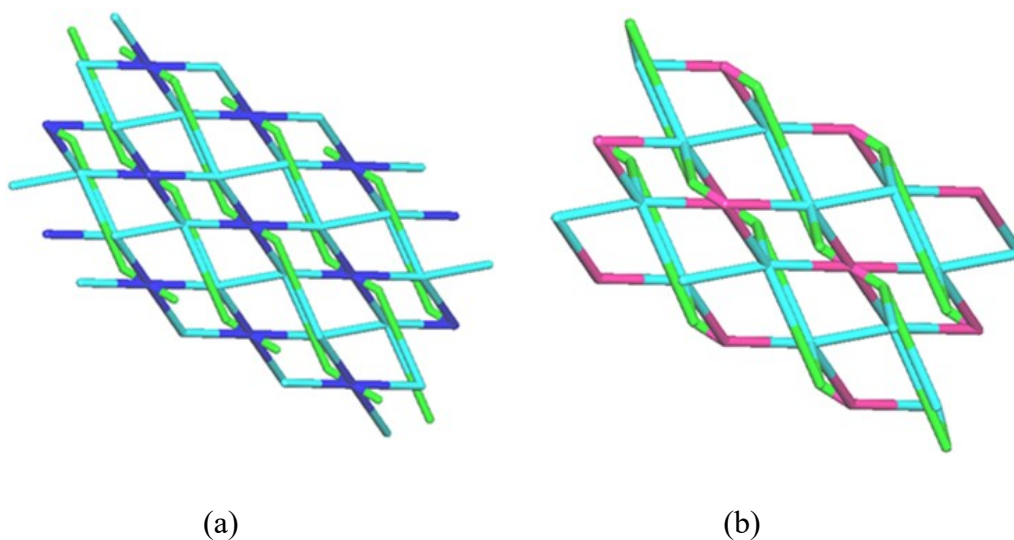
Figure S8. Node-and-linker-type description of the 2D coordination frameworks in **Co-CP** (a: 3,5,6 trinodal net) and **Ni-CP** (b: 2,4,6 trinodal net).

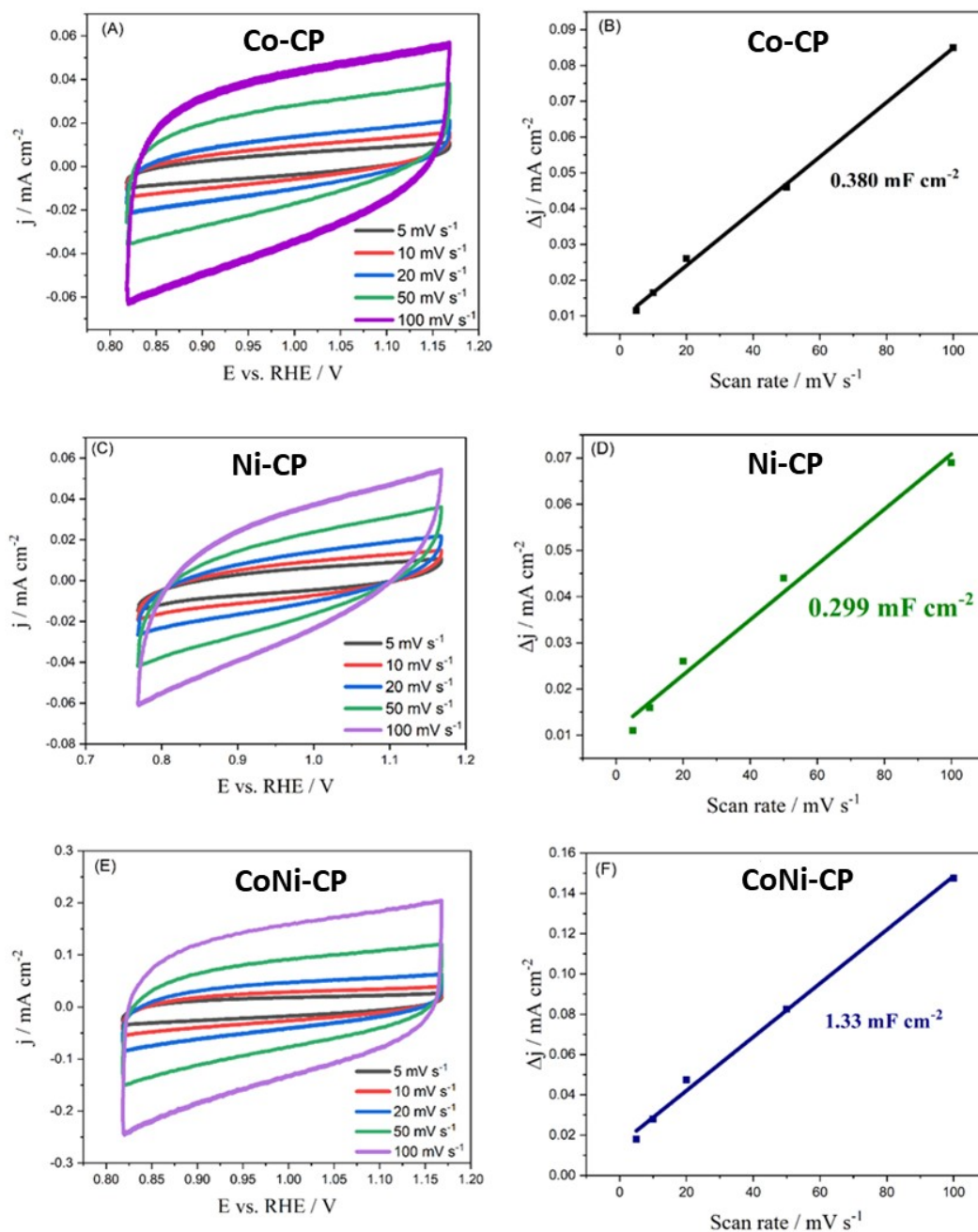**Figure S9**. Capacitance CV plots for **Co-CP**, **Ni-CP** and **CoNi-CP** (a, c, and e respectively), and corresponding difference between cathodic and anodic current density at 0.95 V vs. RHE vs. scan rate (b, d, and f).

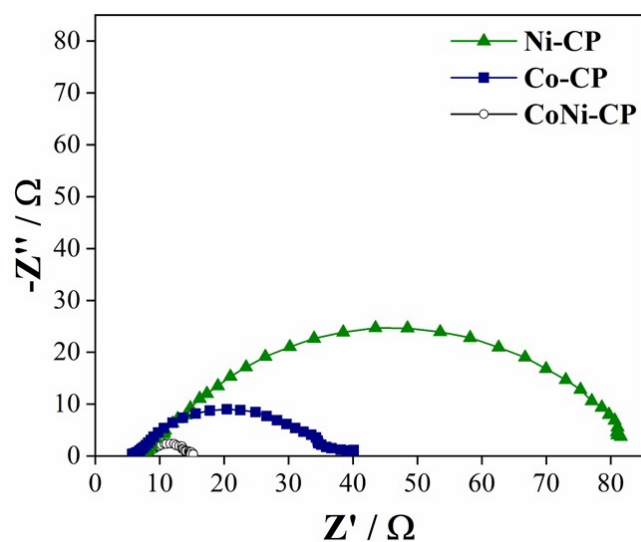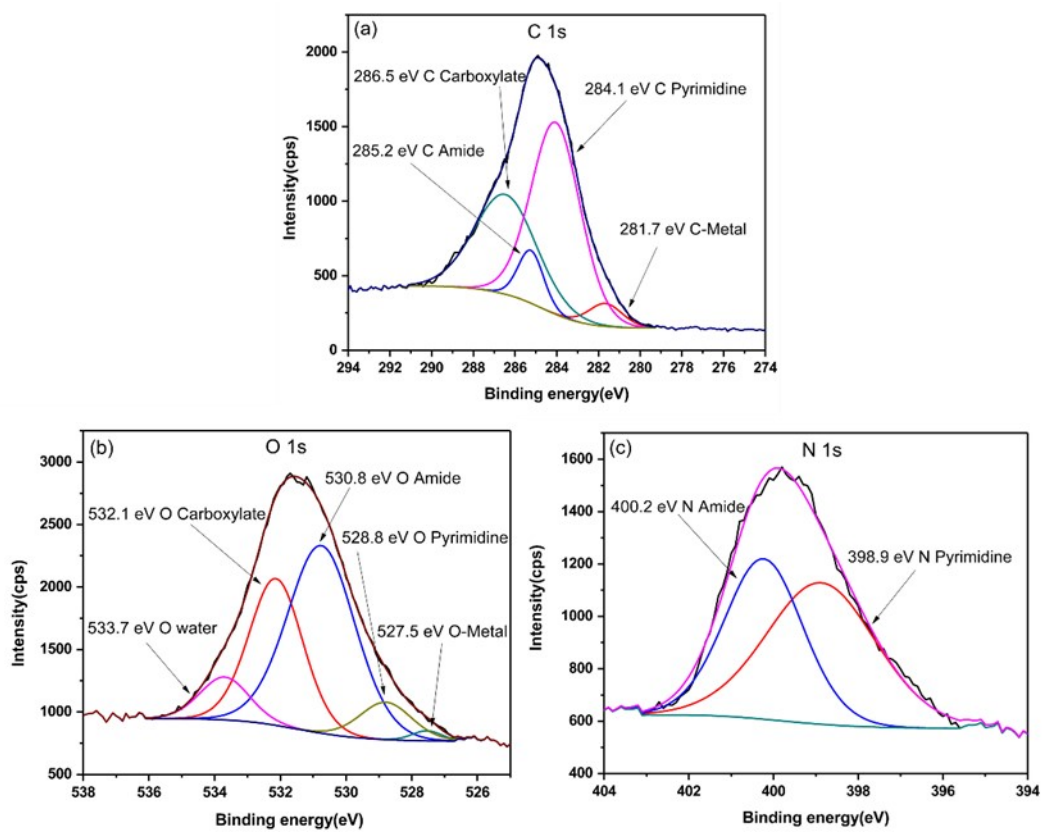**Figure S10**: Nyquist plot of **Co-CP**, **Ni-CP** and **CoNi-CP** at 1.67 V vs. RHE.

Figure S11. High resolution spectra of C 1s (a), O 1s (b) and N 1s (c) for **CoNi-CP**.
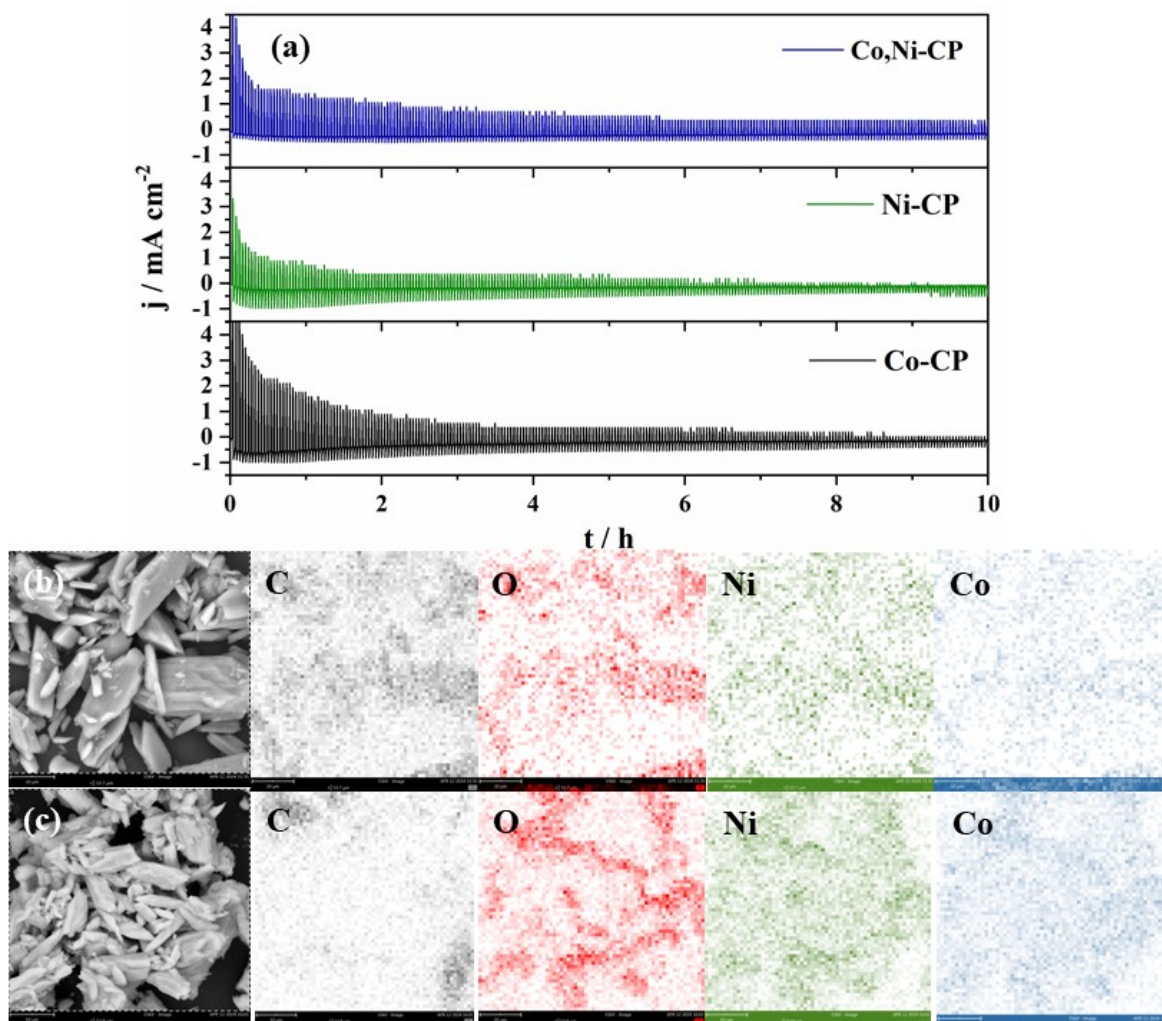
12

Figure S12. Durability study of **Co-CP**, **Ni-CP** and **CoNi-CP** CPs in switch OER/ORR mode (a) with SEM images and elemental mapping of CoNi-CP working electrode before (b) and after (c) the electrochemical tests.

Table S1. Crystallographic data of **Co-CP** and **Ni-CP**.

	Co-CP	Ni-CP
Empirical formula	$C_{24}H_{20}N_6O_8Co$	$C_{24}H_{20}N_6O_8Ni$
Formula weight	579.39	579.17
Crystal system	triclinic	triclinic
Space group	P-1	P-1
a (Å)	7.6976(5)	7.6921(2)
b (Å)	7.8986(5)	7.8232(2)
c (Å)	10.9820(7)	10.9612(3)
α (°)	108.974(3)	108.5190(10)
β (°)	90.541(3)	90.3980(10)
γ (°)	114.662(3)	114.6470(10)
V (Å^3)	565.59(6)	560.99(3)
Z	1	1
ρ_{calc} (g/cm^3)	1.701	1.714
F000	297.0	298.0
μ (mm^{-1})	0.827	0.933
Rfl. measured	26886	22787
Obs/Unique rfl.	2250/2141	2228/2032
Rint	0.0313	0.0536
R(F) (I >=2σ(I))	0.0218	0.0241
wR (F^2) (all data)	0.0238	0.0289
GOF (F^2)	1.118	1.063
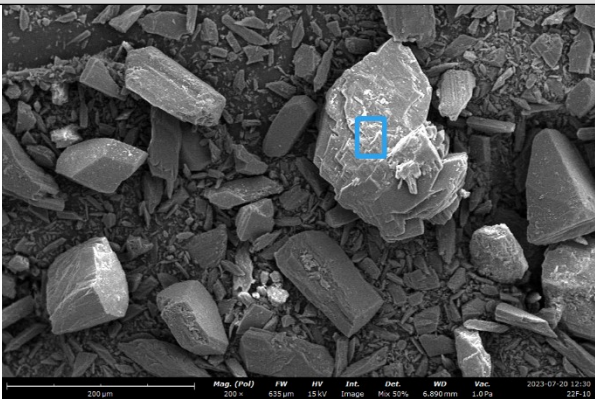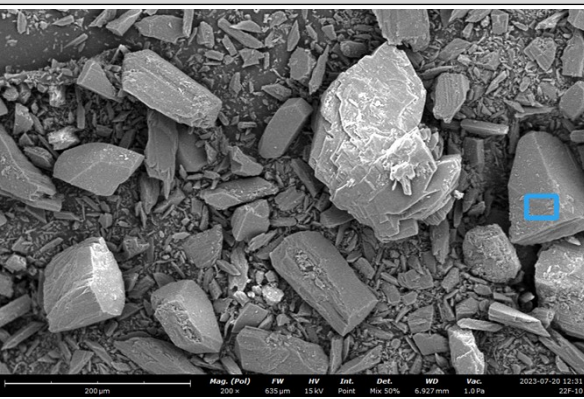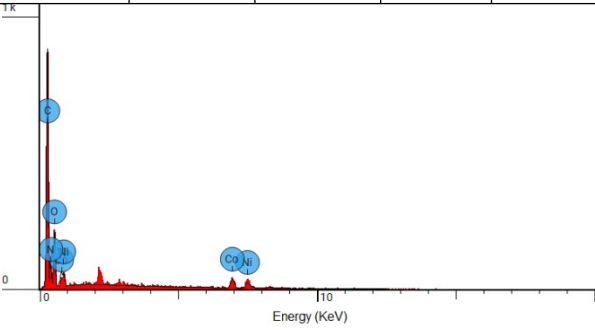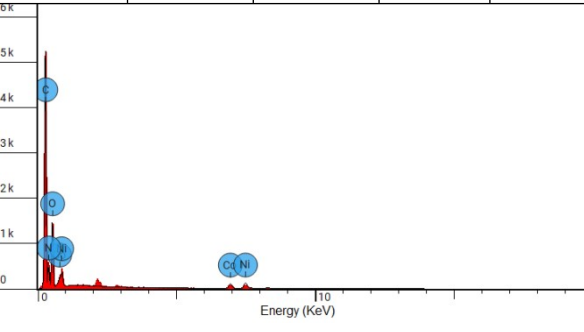
Table S2. Selected bond lengths (Å) and angles (°) in the crystal structure of **Co-CP** and **Ni-CP**.

Metal environment		
	Co-CP (M = Co)	Ni-CP (M = Ni)
M–O$_{water}$	2.1295(11)	2.0731(13)
M–O$_{carboxylate}$	2.0394(10)	2.0376(11)
M–N$_{pyrimidine}$	2.1863(12)	2.1257(13)
<O$_{water}$–M–O$_{carboxylate}$	86.19(5) 93.81(5)	85.96(5) 94.04(5)
<O$_{water}$–M–N$_{pyrimidine}$	89.97(5) 90.03(5)	88.83(5) 91.17(5)
<O$_{carboxylate}$–M–N$_{pyrimidine}$	89.03(4) 90.97(4)	88.52(5) 91.47(5)
Ligand environment		
C=O	1.217(2) 1.245(2) 1.271 (2)	1.214(2) 1.246(2) 1.267(2)
<Ar$_{carboxylate}$···Ar$_{pyrimidin}$	60.52	61.28

Table S3. Geometry (bond lengths in Å and angles in °) of the H-bonds.

	Co-CP			Ni-CP		
	D···A	∠D−H···A	*Symmetry operation (')*	D···A	<D−H···A	*Symmetry operation (')*
O_{water}−H···$N_{pyrimidine}$'	3.051(2)	177(2)	*-1-x,-1-y,1-z*	3.077(2)	175(2)	*x,-1+y,z*
O_{water}−H···$O_{carboxylate}$	3.0047(18)	137(2)	*intra*	2.922(2)	141(2)	*intra*
O_{water}−H···O_{amide}'	2.811(2)	124(2)	*-x,-1-y,1-z*	2.813(2)	118(2)	*-x,1-y,1-z*
N_{amide}−H···$O_{carboxylate}$'	2.931(2)	158.7(18)	*-x,-y,1-z*	2.931(2)	158.2(19)	*-x,2-y,1-z*
$C_{pyrimidine}$−H···$N_{pyrimidine}$	3.467	139.73		3.411	138.37	
$C_{pyrimidine}$−H···$O_{carboxylate(coord)}$	3.200	115.31		3.151	115.92	
$C_{pyrimidine}$−H···O_{amide}' (intra)	2.817(2)	114	-	2.815	114.77	

Table S4. Data of the EDS study of the bimetallic **CoNi-CP**.

Region 1	Region 2

Element Number	Element Symbol	Element Name	Atomic Conc.	Weight Conc.	Element Number	Element Symbol	Element Name	Atomic Conc.	Weight Conc.
6	C	Carbon	47.471	37.200	6	C	Carbon	48.643	39.200
7	N	Nitrogen	30.083	27.500	7	N	Nitrogen	26.274	24.700
8	O	Oxygen	18.200	19.000	8	O	Oxygen	21.889	23.500
27	Co	Cobalt	2.601	10.000	27	Co	Cobalt	1.366	5.400
28	Ni	Nickel	1.645	6.300	28	Ni	Nickel	1.828	7.200

Region 3					Complete map				

Element Number	Element Symbol	Element Name	Atomic Conc.	Weight Conc.	Element Number	Element Symbol	Element Name	Atomic Conc.	Weight Conc.
6	C	Carbon	42.193	33.866	6	C	Carbon	44.116	34.300
7	N	Nitrogen	31.475	29.471	7	N	Nitrogen	30.872	28.000
8	O	Oxygen	23.356	24.975	8	O	Oxygen	20.757	21.500
27	Co	Cobalt	1.243	4.895	27	Co	Cobalt	2.018	7.700
28	Ni	Nickel	1.732	6.793	28	Ni	Nickel	2.237	8.500

Table S5. Comparison of OER kinetic parameters.

Catalyst	Tafel slope (mV dec^{-1})	Overpotential at 10 m Acm^{-2} (mV)	Electrolyte	j_{500} (mA cm^{-2})	Reference
Co-CP	120	422	1 M KOH	29.7	This work
Ni-CP	110	396	1 M KOH	38.3	This work
CoNi-CP	98	416	1 M KOH	40.8	This work
CoNi-NC	89	324	1 M KOH	nd	5
CoNi-BDC-CC	42	251	1 M KOH	nd	6
CoNi@HPA-MOF	58	320	1M KOH	nd	7
CoNiPP	60	246	1 M KOH	nd	8
NiCO$_2$O$_4$	74	360	1 M KOH	nd	9

NC: nitrdetermined. carbon; BDC: 1,4-benzenedicarboxylate; CC: carbon cloth; HPA: hypoxanthine; PP: phenylphosphonates; nd: not determined

References

(1)   *Bruker, APEX2. Bruker AXS Inc., Madison, Wisconsin, USA* **2012**. https://doi.org/10.1039/d2nj06190b.

(2)   Sheldrick, G. M. *SADABS. Program for Empirical Absorption Correction. University of Gottingen, Germany* **2000**. https://doi.org/10.1039/d3nj00279a.

(5)   Sheldrick, G. M. Crystal Structure Refinement with SHELXL. *Acta Crystallogr.* **2015**, *71*, 3–8. https://doi.org/10.1107/S2053229614024218.

(4)   Farrugia, L. J. WinGX and ORTEP for Windows: An Update. *J. Appl. Crystallogr.* **2012**, *45* (4), 849–854. https://doi.org/10.1107/S0021889812029111

(5)   Kumar, G.; Dey, R. S. Coordination Engineering of Dual Co, Ni Active Sites in N-Doped Carbon Fostering Reversible Oxygen Electrocatalysis. *Inorg. Chem. 2023, 62, 33,* 13519–13529. https://doi.org/10.1021/acs.inorgchem.3c01925.

(6)   Bai, X. J.; Chen, H.; Li, Y. N.; Shao, L.; Ma, J. C.; Li, L. L.; Chen, J. Y.; Wang, T. Q.; Zhang, X. M.; Zhang, L. Y.; Fu, Y.; Qi, W. CoNi-Based Metal-Organic Framework Nanoarrays Supported on Carbon Cloth as Bifunctional Electrocatalysts for Efficient Water-Splitting. *New J. Chem.* **2020**, *44* (5), 1694–1698. https://doi.org/10.1039/c9nj06204a.

(7)   Lu, M.; Li, Y.; He, P.; Cong, J.; Chen, D.; Wang, J.; Wu, Y.; Xu, H.; Gao, J.; Yao, J. Bimetallic Metal-Organic Framework Nanosheets as Efficient Electrocatalysts for Oxygen Evolution Reaction. *J. Solid State Chem.* **2019**, *272*, 32–37. https://doi.org/10.1016/j.jssc.2019.01.023.

(8)   Feng, P.; Cheng, X.; Li, J.; Luo, X. Calcined Nickel-Cobalt Mixed Metal Phosphonate with Efficient Electrocatalytic Activity for Oxygen Evolution Reaction. *ChemistrySelect* **2018**, *3* (2), 760–764. https://doi.org/10.1002/slct.201702637.

(9)   Broicher, C.; Zeng, F.; Artz, J.; Hartmann, H.; Besmehn, A.; Palkovits, S.; Palkovits, R. Facile Synthesis of Mesoporous Nickel Cobalt Oxide for OER – Insight into Intrinsic Electrocatalytic Activity. *ChemCatChem* **2019**, *11* (1), 412–416. https://doi.org/10.1002/cctc.201801316.